

# Measurement and identification of the vibration characteristics of motorcycle riders

V. Cossalter, A. Doria, D. Fabris, M. Maso

Department of Mechanical Engineering – Padova University

Via Venezia 1, 35131 Padova Italy

e-mail: [alberto.doria@unipd.it](mailto:alberto.doria@unipd.it)

## Abstract

This paper shows the experimental responses of five riders to roll and steer oscillations. The analysis is carried out to identify the properties of a rider multi-body model, which can be useful for simulation. The riders have different physiques and riding experience and are excited by means of the motorcycle riding simulator developed at DIM. A stepped sine testing is performed. The results of the steer tests are presented in terms of FRFs between the angular acceleration of the steer and the steering torque. A multi-body model is used to fit the experimental data. The results of the roll tests are presented in terms of FRFs between the accelerations measured at three point of the body of the rider (head, shoulders, torso) and the acceleration of a point placed at a fixed distance from the oscillation axis. To clarify the dynamic response of the rider, a relative motion FRF is calculated as well: it is the ratio between the relative tangential acceleration and the acceleration at the same point caused only by the roll angular acceleration.

## 1 Introduction

The most important features of two-wheeled vehicles are handling, stability and comfort. They depend on the mechanical characteristics of the vehicle (e.g. steering system kinematics, mass distribution, tire properties) but also on the dynamic properties of the bodies of the rider and passenger, because the ratio between the mass of the passengers and the mass of the vehicle is not as small as in other kinds of vehicles. Hence, the rider influences the behavior of the vehicle not only through the voluntary control actions, but also through the passive behavior of his/her body, which responds to the motion imposed by the vehicle. This paper focuses on the passive behavior of the rider.

The properties of the human body can be divided into rigid-body properties and multi-body/vibration properties. They have to be taken into account in the development of vehicle's models for numerical simulation and in the analysis of experimental results. Rigid-body properties are calculated assuming that the human body behaves as a rigid body. These properties are the mass, the center of mass location and the moments of inertia. An extensive review of rigid-body properties can be found in [1].

The rigid-body properties of the human body are enough to perform many handling simulations [2] and to analyze the most important features of stability [3] and comfort [4]. Nevertheless, more detailed simulations require a multi-body model of the rider. In particular some papers present results that take into account the lateral mobility of the rider [5], but the impedance of the handle-bars caused by the rider is neglected (in other words the stability analysis is carried out assuming free handle-bars). In multi-body models the human body is represented by a system of rigid bodies (one for each limb) connected by joints, which simulate the articulations and have stiffness and damping properties [6]. The multi-body model of the rider possesses natural frequencies and damping properties that simulate the actual vibration properties of the human body. This paper deals with the measurement and identification of the vibration characteristics of motorcycle riders, in order to make possible the development of advanced multi-body models of the vehicle with the rider.

The measurement of the passive response of the rider's body to forced oscillations of the handle-bars and of the whole motorcycle is particularly important because two-wheeled vehicles in motion are characterized by modes of vibration (weave, wobble), which in certain conditions become unstable [7][8]. Since the natural frequencies of these modes (2÷4 Hz for weave, 4÷10 Hz for wobble) are too high to be controlled by the rider's voluntary actions (especially wobble), the passive effect of the rider body may represent an important source of stabilization.

These phenomena are similar to the aircraft-pilot coupling (APC) problems, which have been found in some aircrafts [9][10] and have frequencies in the range 0.5÷3 Hz. APC problems are generated by the aircraft lateral and roll accelerations at the pilot's position that influence the pilot control input through the inertial forces of the limbs of the pilot and the inceptor.

The first part of this paper deals with the experimental study of the response of the rider to handle-bars oscillations in the range 0.5÷10 Hz. The second part of the paper focuses on the experimental study of the response of the rider's body to roll oscillations of the whole motorcycle.

## 2 Testing equipment

The rider is excited by means of the motorcycle riding simulator developed by the Department of Mechanical Engineering (DIM) of Padova University for the study of safety and maneuverability of two wheeled vehicles. It consists of a serial kinematic chain (three mobile interlinked members) that moves a motorcycle mock-up and that generates motion cues during riding, see figure 1. The system permits three principal rotation of the rider (yaw, roll and pitch) and lateral displacement. The axes are driven by brush-less servomotors, the rotations and velocities are measured by means of encoders. A servomotor is fitted to the steer axis and generates torques similar to the ones experienced by the rider on the road.



**Figure 1: Motorcycle riding simulator.**

For this particular research only the roll and the steer servomotors are used for exciting the body of the rider. A stepped-sine testing is used. The amplitude and frequency step are chosen at the beginning of the test. The control program for a defined testing interval generates a single frequency sine wave and then it passes to the subsequent frequency.

The steering torque is measured by a torsionmeter mounted between the steer servomotor and the handle-bars. During the tests, the steering system of the simulator was upgraded and consequently two different kinds of torsionmeter were used. The first torsionmeter was composed by a shaft equipped with strain gages that measured directly the torque. The shaft was coaxial with the servomotor axis. The present torsionmeter uses a little bar (equipped with strain gages) mounted in radial direction that connects the servomotor shaft with the mobile plate fixed to the handle-bars. The rotation of the handle-bars is measured by a rotational potentiometer.

### 3 Rider’s response to steer excitation

#### 3.1 Experimental results

The tests are carried out according to the following procedure. The tester rides the motorcycle mock-up of the simulator and holds the handle-bars. The axes of the simulator are locked except the steer axis. The steer servomotor generates a stepped-sine excitation with constant amplitude (4°) and increasing frequency in the range 0.5÷8.5 Hz with increments of 0.5 Hz. Some testers with different physiques and riding experience participate in the research program, their features are summarized in table 1.

Rider	Height [cm]	Mass [kg]	Riding experience
1	176	81	10
2	169	56	2
3	188	86	2
4	177	74	6
5	170	63	7

Table 1: Riders’ characteristics

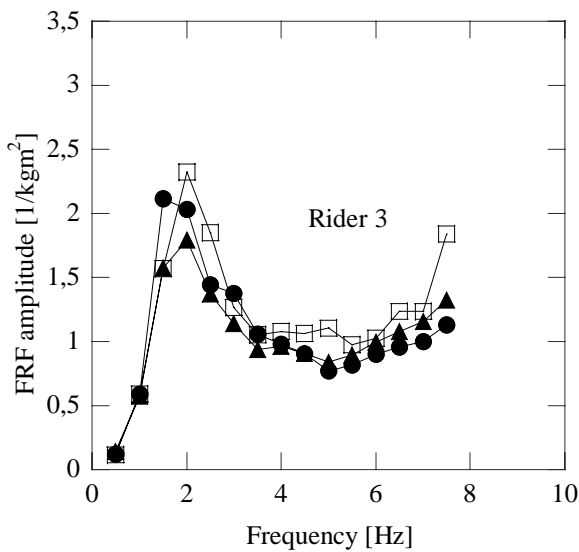


Figure 2: Steer test repeatability, amplitudes of the FRFs.

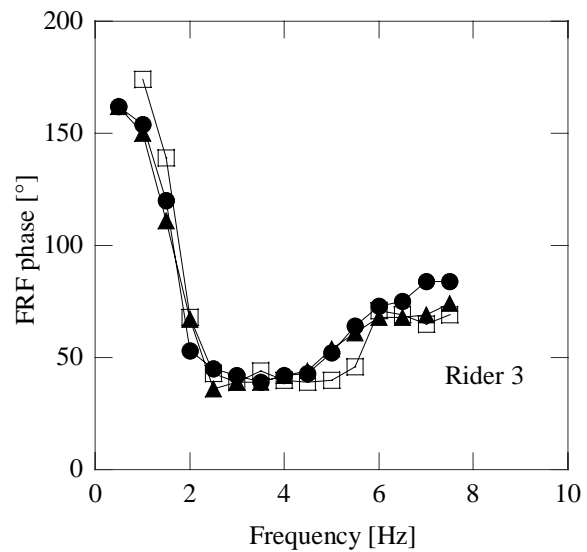


Figure 3: Steer test repeatability, phases of the FRFs.

During the tests, the time records of the steering torque generated by the servomotor and the rotation of handle-bars are collected. Then, the frequency response function (FRF) is calculated: it is the ratio between the cross-spectrum of angular acceleration and steering torque and the auto-spectrum of the steering torque.

The experimental results obtained with the same rider show good repeatability both in terms of amplitudes and phases of the FRFs. Figure 2 and 3 show three FRFs (amplitude and phase) of the same rider, obtained at different times and with the two different versions of the torsionmeter. All the amplitude curves present the same shape with a resonance peak at 1.5-2 Hz, a minimum in the interval 4-6 Hz and then increasing values. The phases show high values ( $\approx 160^\circ$ ) at low frequencies, a minimum ( $40^\circ$ ) in the range 2-4 Hz, and then increasing values at high frequencies.

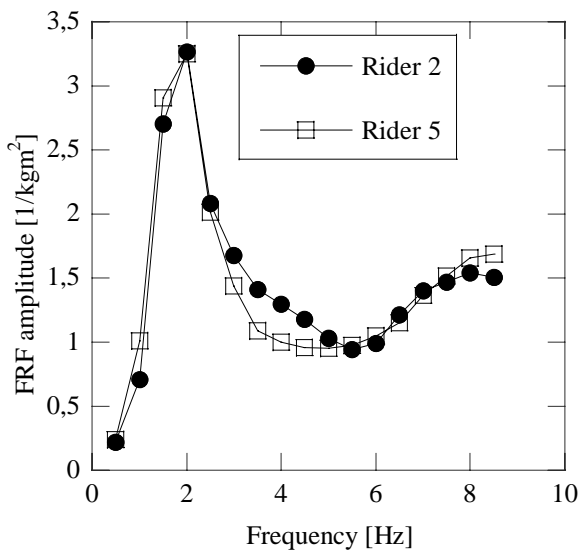


Figure 4: Steer test, amplitudes of the FRFs of two riders.

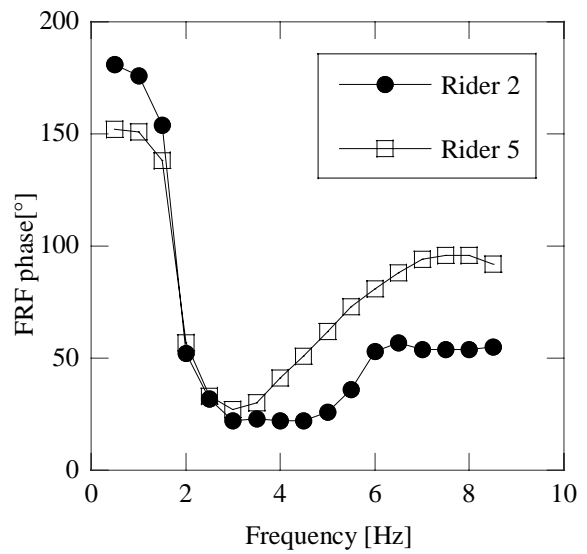


Figure 5: Steer test, phases of the FRFs of two riders.

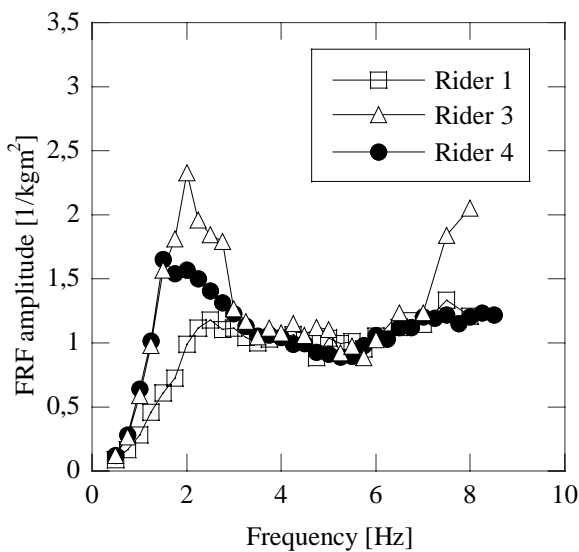


Figure 6: Steer test, amplitudes of the FRFs of three riders.

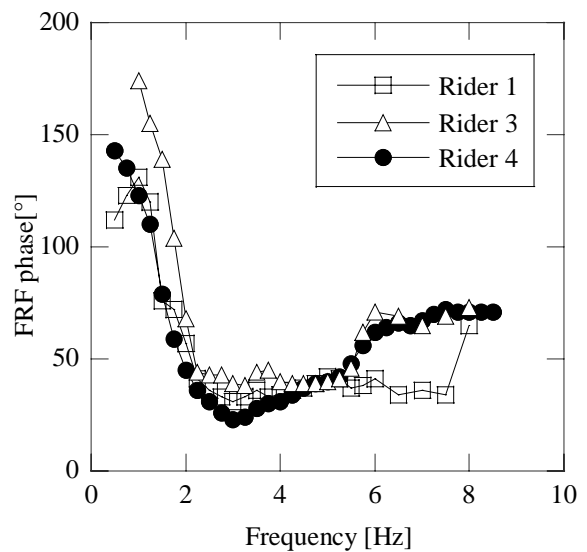


Figure 7: Steer test, phases of the FRFs of three riders.

It's interesting to overlap the results obtained with different riders. All the amplitude plots present the same form with a peak, a minimum zone and then increasing values. The phase plots show high values at low frequencies, a minimum zone, and then increasing values at high frequencies.

In figures 4-5 the experimental data that refer to the smaller riders are presented, they have the highest peak values (low values of the steering torque). The greatest differences between the riders of this group are in terms of phase at the high frequencies. A possible cause of these differences is the different riding experience of each rider: rider 2 has no-experience, rider 5 has a good experience.

In figures 6-7 the experimental data that refer to the more robust riders are presented; they exert steering torques that, in resonance condition, are higher than the ones exerted by the riders of the other group. In the range of medium and high frequencies the differences between the two groups of riders are smaller.

### 3.2 Identification

Figure 8 shows a scheme of the multi-body model for the analysis of rider's response to steer excitation. There are a fixed frame and six moving rigid bodies: the handle-bars, torso of the rider, left and right arms, left and right forearms. The articulations are simulated by means of joints, like in [6]. A spherical pair simulates the articulation of the shoulder, a revolute pair simulates the articulation of the elbow and a couple of revolute pairs simulates the articulation of the wrist. The waist rotation about an axis joining the pelvis with the head is simulated by means of a revolute pair. The hands are assumed to be firmly attached to the handle-bars. Finally there is the revolute pair of the steer. The system has 2 degree-of-freedom, the generalized coordinates are steer rotation  $\theta_s$  and torso rotation  $\theta_t$ . The elastic and damping properties of the systems are represented by visco-elastic springs that connect the limbs and by a visco-elastic torsion spring that connects the torso with the frame. Torque  $M_s$  is generated by the servomotor about the steer axis. If large displacements are considered the system exhibits a non linear behavior, caused by non linear kinematic equations.

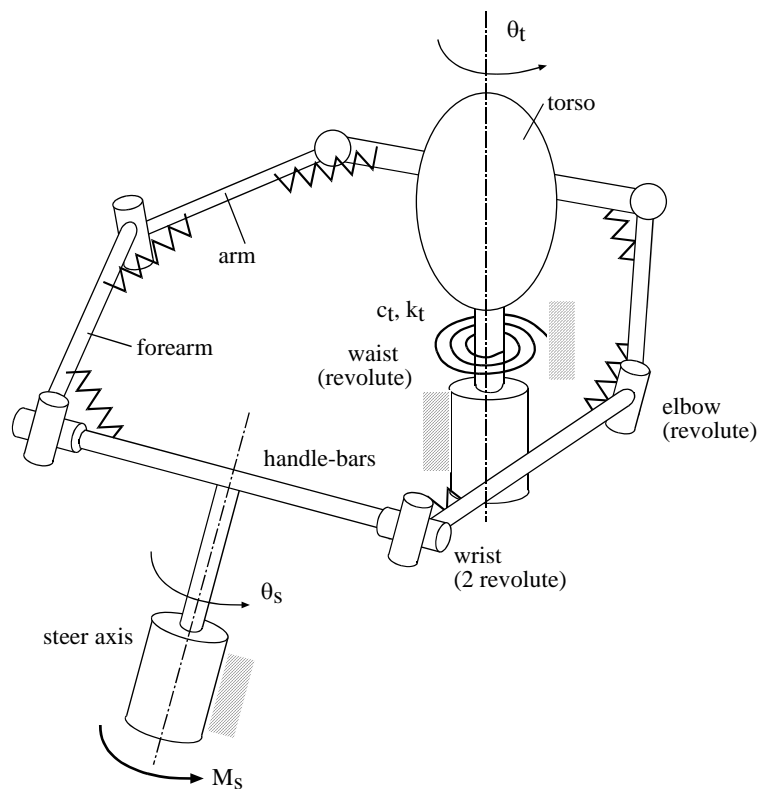


Figure 8: Multi-body model of the rider-steer system.

The Lagrange equations of this system are:

$$\frac{d}{dt} \left( \frac{\partial T}{\partial \dot{\theta}_s} \right) - \frac{\partial T}{\partial \theta_s} = Q_{s-el} + Q_{s-visc} + Q_{s-g} + M_s \quad (1)$$

$$\frac{d}{dt} \left( \frac{\partial T}{\partial \dot{\theta}_t} \right) - \frac{\partial T}{\partial \theta_t} = Q_{t-el} + Q_{t-visc} + Q_{t-g} - c_t \dot{\theta}_t - k_t \theta_t \quad (2)$$

In which  $T$  is the kinetic energy. The generalized torques associated with the generalized coordinate  $\theta_s$  are: the elastic and viscous torques of the visco-elastic springs ( $Q_{s-el} + Q_{s-visc}$ ), the gravity torque ( $Q_{s-g}$ ) and torque  $M_s$ , which acts directly on the steer axis. The generalized torques associated with generalized coordinate  $\theta_t$  are: the elastic and viscous torques of the visco-elastic springs ( $Q_{t-el} + Q_{t-visc}$ ), the gravity torque ( $Q_{t-g}$ ) and the viscous and elastic torques of the torsion spring ( $-c_t \dot{\theta}_t, -k_t \theta_t$ ), which act directly on the waist joint.

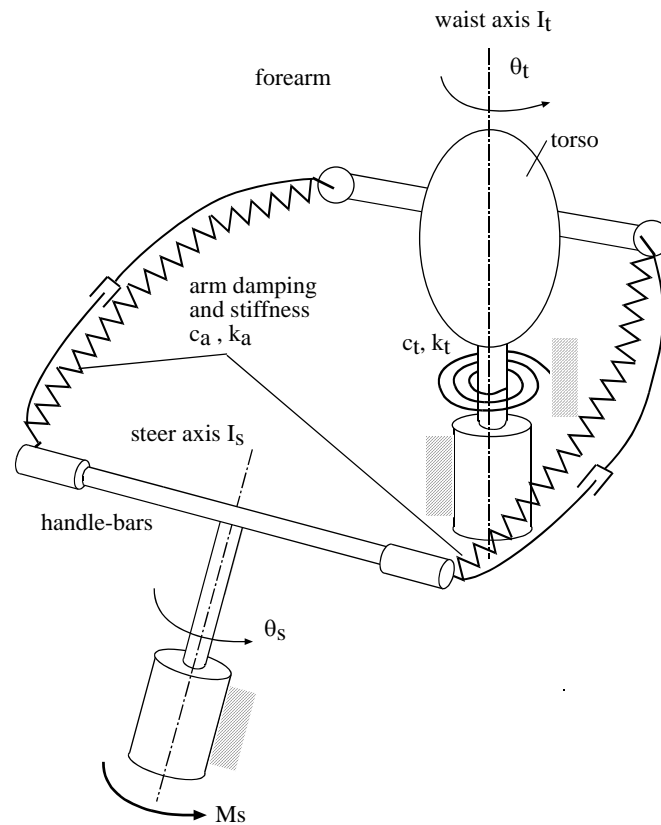


**Figure 9: Simplified multi-body model of the rider-steer system.**

If only small oscillations are considered, the equations of motion can be linearized and become:

$$I_s \ddot{\theta}_s + I_{cc} \ddot{\theta}_t = -c_a (\dot{\theta}_s - \dot{\theta}_t) - k_a (\theta_s - \theta_t) + M_s \quad (3)$$

$$I_{cc} \ddot{\theta}_s + I_t \ddot{\theta}_t = -c_a (\dot{\theta}_t - \dot{\theta}_s) - k_a (\theta_t - \theta_s) - c_t \dot{\theta}_t - k_t \theta_t \quad (4)$$

The moment of inertia  $I_s$  includes the moment of inertia of the handle-bars and a share of the moment of inertia of the forearms. The moment of inertia  $I_t$  includes the moment of inertia of the torso and a share of the moment of inertia of the arms.  $I_{cc}$  is the cross-coupling moment of inertia that depends on the masses

of arms and forearms, it will be neglected with respect to  $I_s$  and  $I_t$ .  $c_a$  is an equivalent damping coefficient of arms, whereas  $k_a$  is an equivalent stiffness coefficient of the arms. The gravity forces are neglected since the axes of rotation are almost vertical. The linearized model can be represented by the scheme of figure 9.

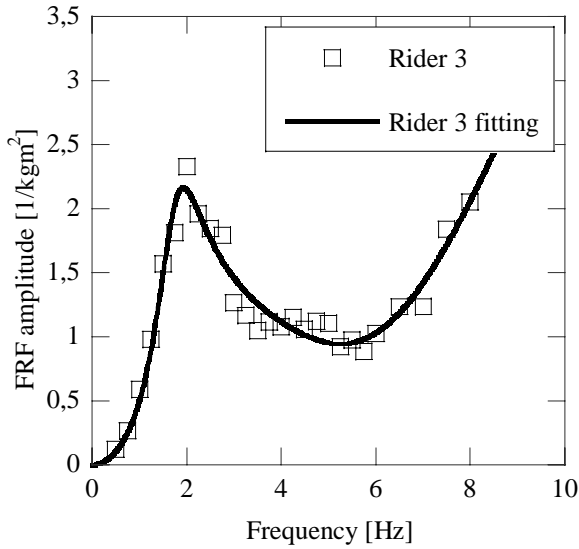


Figure 10: Rider 3, optimum fitting of experimental results, amplitude.

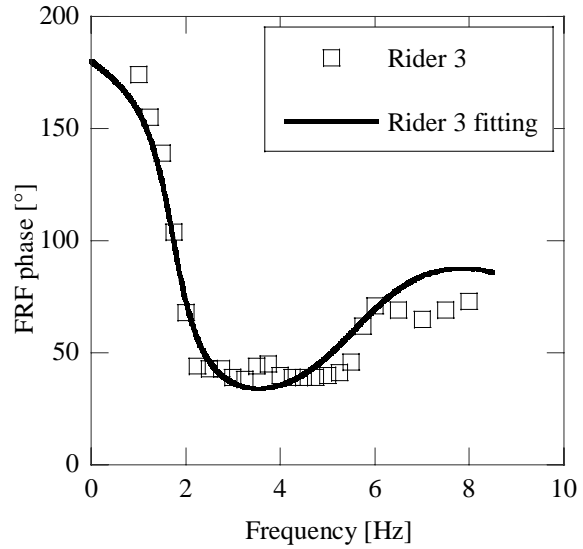


Figure 11: Rider 3, optimum fitting of experimental results, phase.

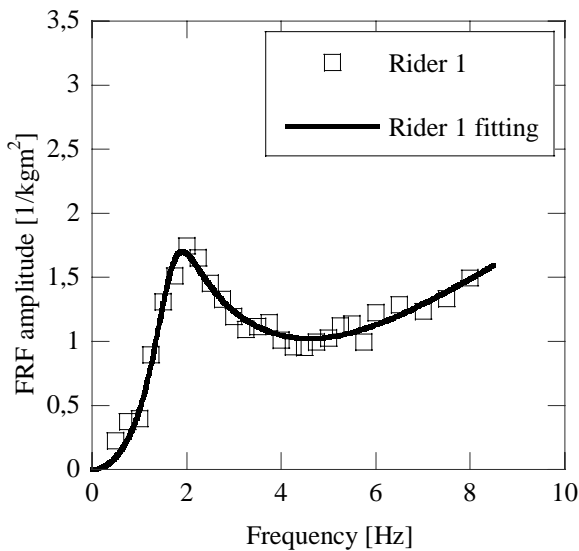


Figure 12: Rider 1, optimum fitting of experimental results, amplitude.

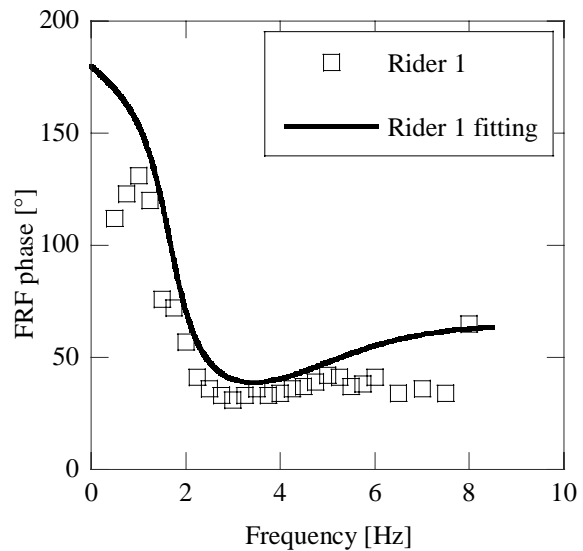


Figure 13: Rider 1, optimum fitting of experimental results, phase.

Equation (3) and (4) are enough for linear analysis and can be easily implemented in a multi-body model of the motorcycle and rider for the analysis of stability. If a harmonic oscillation (with angular frequency  $\omega$ ) is commanded by the steer servomotor, from equations (3) and (4) the analytical FRF between the steer angular acceleration and the steer torque can be derived:

$$\frac{\ddot{\theta}_s(\omega)}{M_s(\omega)} = -\frac{(-\omega^2 I_t + i\omega(c_a + c_t) + k_a + k_t)\omega^2}{-(i\omega c_a + k_a)^2 + (-\omega^2 I_s + i\omega c_a + k_a)(-\omega^2 I_t + i\omega(c_a + c_t) + k_a + k_t)} \quad (5)$$

Equation (5) is useful for fitting experimental results and for identifying the biomechanical properties of the rider.

Optimum fitting of experimental data is carried out by means of a Matlab code, which looks for the six biomechanical parameters ( $I_s, I_t, c_a, c_t, k_a, k_t$ ) that minimize (in the least-squares sense) the difference between the amplitude of the experimental FRF and the amplitude of the model FRF (equation 5). Results dealing with rider 3 are presented in figures 10 and 11. Even if the optimum fitting is carried out considering only the amplitude, the results are satisfactory both for the amplitude and the phase. Figures 12 and 13 show the results of optimum fitting for rider 1.

Table 2 summarizes the values of the identified biomechanical parameters of some riders

Rider	$I_s$ (kgm <sup>2</sup> )	$I_t$ (kgm <sup>2</sup> )	$k_a$ (Nm/rad)	$k_t$ (Nm/rad)	$\nu_1$ (Hz)	$\nu_2$ (Hz)	$\zeta_1$ (%)	$\zeta_2$ (%)
1	0.200	0.842	820	127	1.74	-	31	> 1
2	0.261	0.592	809	100	1.71	10.7	15	70
3	0.252	0.664	796	118	1.80	10.6	28	40
4	0.193	0.810	1100	96	1.56	-	32	> 1
5	0.150	0.736	783	102	1.70	12.6	12	92

**Table 2: Identified biomechanical parameters of some riders.**

Moment of inertia  $I_s$  is comprehensive of forearms and of handle-bars ( $\approx 0.12$  kgm<sup>2</sup>). Natural frequencies  $\nu_1, \nu_2$  and damping ratios  $\zeta_1, \zeta_2$  are the modal parameters of the whole system.

The identified parameters are compatible each other and with the data that are present in literature. In particular, if the ratios between the masses of the different subjects are taken into account, the values of moment of inertia  $I_t$  (about the waist axis) are similar to the one presented in [6]. Also the values of waist stiffness  $k_t$  are very similar to the one presented in [6].

## 4 Rider's response to roll excitation

### 4.1 Experimental results

The tests are carried out according to the following procedure. The tester rides the motorcycle mock-up of the simulator and holds the handle-bars, he is instructed to look at a fixed point during the test. The axes of the simulator are locked except the roll axis. The roll servomotor generates a sinusoidal motion with constant amplitude ( $1^\circ$ ) and frequency. Series of tests are performed in the frequency range  $0.5\div 7$  Hz with increments of 0.25 Hz. The sequence of test frequencies is chosen randomly, to avoid voluntary reactions of the test rider.

The measurement system includes four piezo-electric accelerometers. The first accelerometer is mounted at point  $P_1$  of the motorcycle mock-up at distance  $h_1$  from point  $O$  on the roll axis (see figure 14). It measures the tangential acceleration caused by the roll oscillation:

$$\vec{a}_{t1} = \vec{\alpha} \times OP_1 \tag{6}$$

in which  $\vec{\alpha}$  is the angular acceleration. In component form:

$$a_{t1} = \alpha h_1 \tag{7}$$

From the value of  $a_{t1}$  the tangential acceleration of every point  $P_i$  belonging to the rigid plane rotating with angular acceleration  $\alpha$  around the roll axis can be calculated:

$$\alpha h_i = \frac{a_{t1}}{h_1} h_i \tag{8}$$

in which  $h_i$  is the distance of point  $P_i$  from the roll axis (see figure 14).

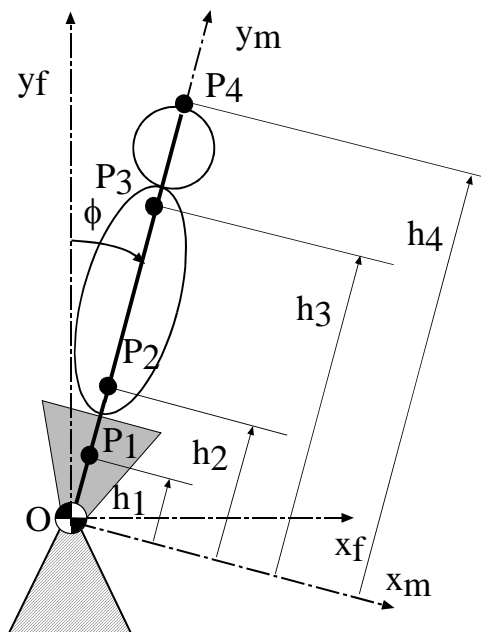


Figure 14: Scheme of roll excitation.

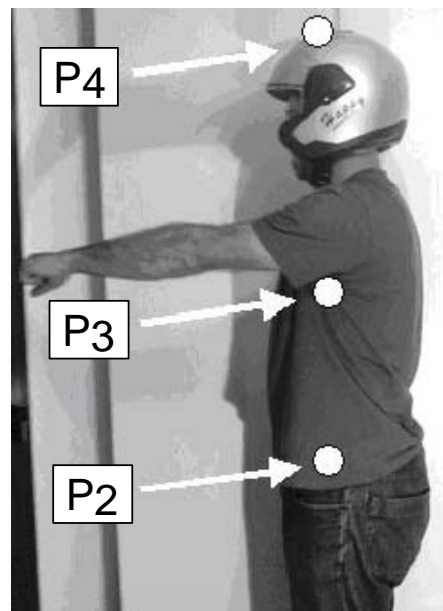


Figure 15: Positions of accelerometers.

The second accelerometer is fixed to the torso of the rider near the waist (see figure 15) by means of a belt. The third accelerometer is fixed (by means of a belt) to the torso of the rider, below the shoulders

(see figure 15), it measures the tangential acceleration. The last accelerometer is mounted on the helmet and measures the tangential acceleration of the head (figure 15).

The tangential accelerations in the points of the rider's body depend both on the forced roll oscillation and on the passive response of the rider body. Actually, if a moving tern  $(x_m, y_m, z_m)$  that rolls with the motorcycle mock-up and has origin in point  $O$  on the roll axis is considered, the following equation holds:

$$\vec{a}_i = \vec{a}_O + \vec{\alpha} \times OP_i + \vec{\omega} \times (\vec{\omega} \times OP_i) + 2\vec{\omega} \times {}^{rel}\vec{v}_i + {}^{rel}\vec{a}_i \quad (9)$$

In which  $\vec{\omega}$  is angular velocity,  ${}^{rel}\vec{v}_i$  relative velocity and  ${}^{rel}\vec{a}_i$  relative acceleration. The term  $\vec{a}_O$  is zero, since point  $O$  is fixed. The term  $\vec{\omega} \times (\vec{\omega} \times OP_i)$  is the radial component of acceleration and does not influence the tangential acceleration measured by the accelerometer. If the velocity of the rider's body relative to the moving frame is assumed to have the tangential direction, the Coriolis term  $(2\vec{\omega} \times {}^{rel}\vec{v}_i)$  is perpendicular to the tangential direction. Hence, the component in the tangential direction of equation (9) becomes:

$$a_{ii} = \alpha h_i + {}^{rel}a_{ii} = \frac{a_{r1}}{h_1} h_i + {}^{rel}a_{ii} \quad (10)$$

The last equation shows that the tangential component of the acceleration measured by the accelerometer on the rider's body depends both on the forced roll acceleration and on the acceleration relative to the tern that moves with the motorcycle mock-up.

In order to study the response of the rider's body the following frequency response function (FRF) is introduced:

$$FRF_i = \frac{a_{ii}}{\frac{a_{r1}}{h_1} h_i} \quad (11)$$

It is the ratio between the tangential component of the acceleration measured by the accelerometer at point  $P_i$  and the acceleration of the same point caused only by the roll angular acceleration.

The tests are carried with three riders, whose characteristics are summarized in table 1.

Figures 16 and 17 show the amplitudes and phases of the FRFs calculated from the accelerations measured at the torso near the waist ( $FRF_2$ ). Even if the three riders have different physiques, the FRFs are rather similar. The largest amplitudes appear at low frequencies and there is a resonance at about 1 Hz, then the amplitudes decreases monotonically with frequency. The phase lag at low frequency is small ( $<45^\circ$ ) and increases when frequency increases.

The FRFs calculated from the accelerations measured at the torso near the shoulders ( $FRF_3$ ) are represented in figures 18 and 19 and are similar for the three riders. If the plot of amplitudes (figure 18) is compared with figure 16 significant differences appear. Figure 18 shows a resonance at about 1 Hz, then the amplitude strongly decreases with frequency, with values in the range  $0.1 \div 0.2$ . Hence, the passive response of the rider's body to the roll excitation is characterized by a motion relative to the motorcycle mock-up, which tends to minimize the tangential acceleration.

Figures 20 and 21 deal with the FRFs calculated from the accelerations measured at the head ( $FRF_4$ ). In this case larger differences between the testers appear. Perhaps the motion of the head is more influenced by the voluntary control of the rider.

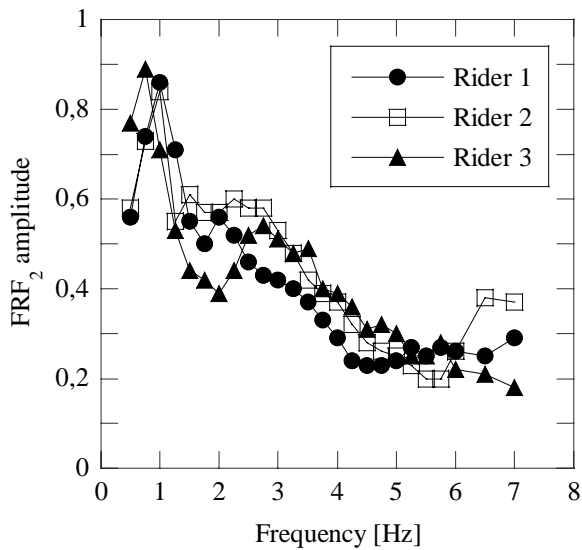


**Figure 16: Amplitudes of the FRF measured at the torso near the waist.**

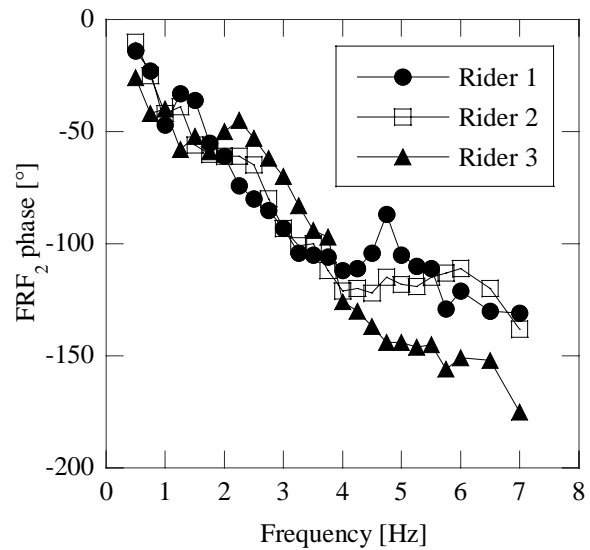


**Figure 17: Phases of the FRF measured at the torso near the waist.**

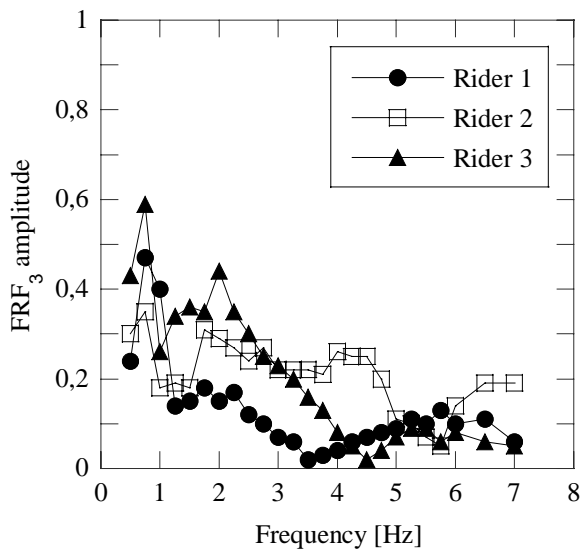


**Figure 18: Amplitudes of the FRF measured at the torso near the shoulders.**

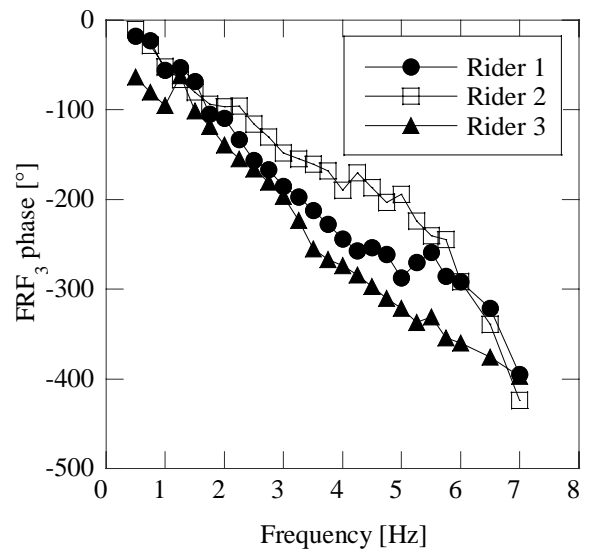


**Figure 19: Phases of the FRF measured at the torso near the shoulders.**

The amplitudes reach the maximum values at low frequency (below 2 Hz) and two peaks appear. Then for riders 1 and 3 the amplitudes decrease sharply and reach values lower than 0.1. Therefore, the rider's head tends to stay firm in spite of the roll motion of the motorcycle mock-up.

For the second rider the amplitude at high frequency does not decrease very sharply. The plot of phases (figure 21) shows for all the riders a phase lag that increases with frequency with a large rate. The plot of rider 2 shows a large phase variation above 5 Hz.

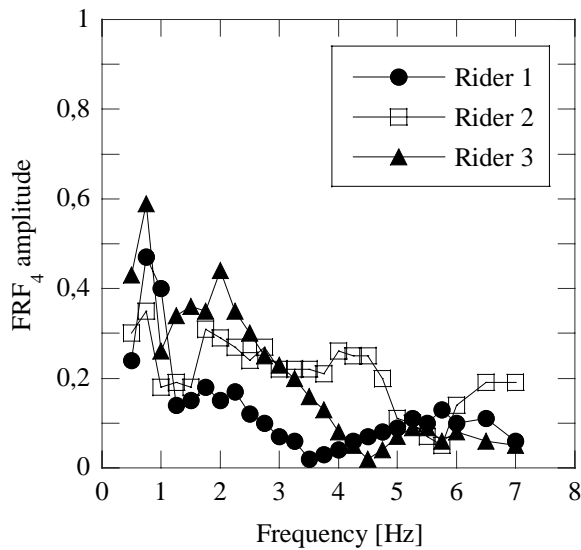


Figure 20: Amplitudes of the FRF measured at the head.

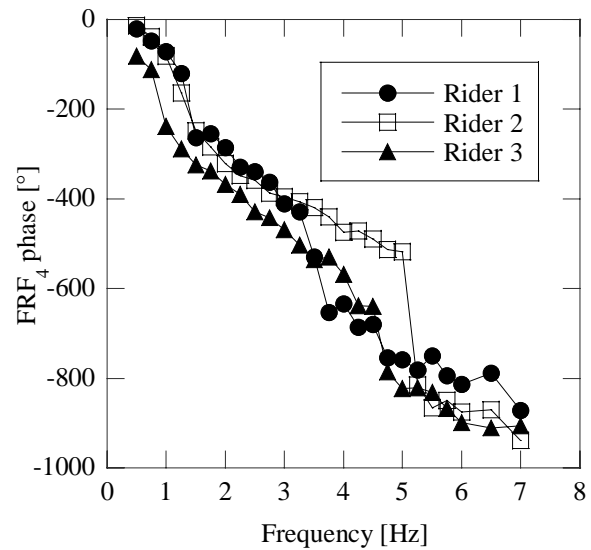


Figure 21: Phases of the FRF measured at the head.

## 4.2 Analysis of results

In order to have a better insight into the dynamic response of the rider's body a new FRF is calculated: the relative motion frequency response function  $rFRF$ . It is the ratio between the relative tangential acceleration, which can be calculated from equation (10) and the acceleration of the same point that is caused only by the roll angular acceleration.

$$rFRF_i = \frac{\frac{rel}{h_1} a_{ti}}{\frac{a_{r1}}{h_1} h_i} = \frac{a_{ti} - \frac{a_{r1}}{h_1} h_i}{\frac{a_{r1}}{h_1} h_i} = FRF_i - 1 \quad (12)$$

Figures 22 and 23 show the amplitudes and phases of the relative motion FRFs for the points on the body of rider 3.

The relative motion FRFs of the torso ( $rFRF_2$  and  $rFRF_3$ ) at low frequency have the smallest values and then increase with frequency reaching values in the range  $1 \div 1.2$  when the frequency is larger than 2 Hz. The relative motion FRF of the head ( $rFRF_4$ ) is small at low frequency, then shows a maximum at 1.25 Hz and reaches a constant value ( $\approx 1$ ) above 2 Hz. The phases of the  $rFRFs$  show some variations in the low frequency range and then have a stable value between  $-150^\circ$  and  $-190^\circ$ . Therefore these plots show that above 2 Hz the relative acceleration, which is caused by the passive response of the rider's body, is large and almost in opposition with the tangential acceleration caused by the roll motion of the motorcycle mock-up. Similar results can be obtained by analyzing the data of the other riders.

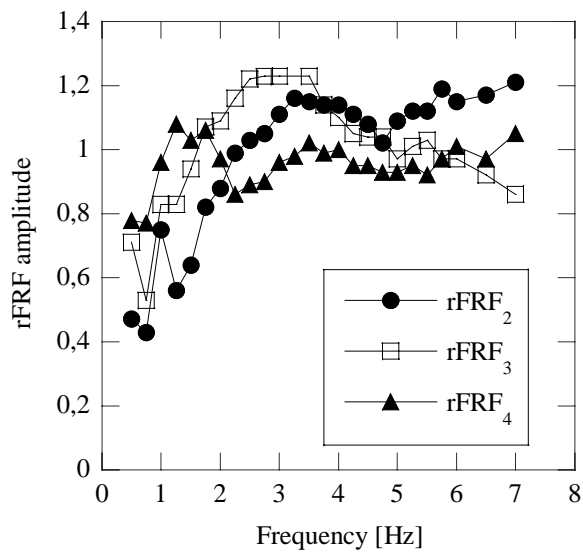


Figure 22: Amplitudes of the relative FRFs of rider 3.

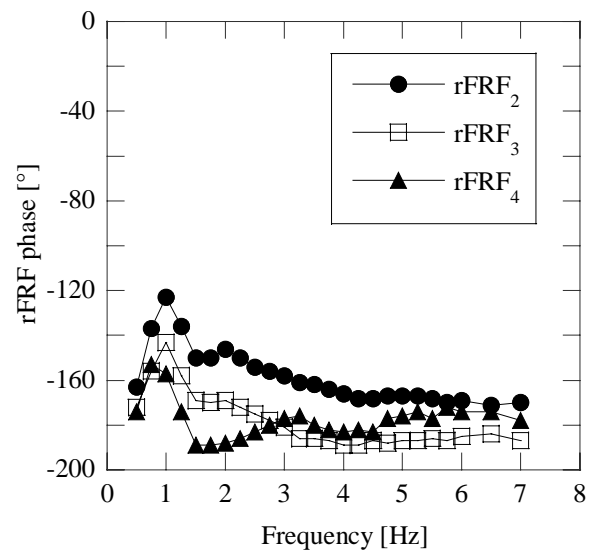


Figure 23: Phases of the relative FRFs of rider 3.

## 5 Conclusions

The motorcycle riding simulator of DIM is useful for studying man-machine interaction in safety conditions with a good repeatability of results. The passive response of some riders to steer excitation show a resonance peak at low frequency (2 Hz) and an increase of the response amplitude at about 6 Hz, which may influence the wobble instability. The passive response of riders to roll excitation shows a peak at very low frequency (about 1 Hz) and then decreasing values. Actually the rider's motion relative to the motorcycle tends to minimize tangential accelerations. The experimental results obtained in the framework of this research will be used in a forthcoming paper that will deal with stability analysis of a motorcycle taking into account the impedance of the rider about the steer axis.

## Acknowledgement

This research was partially supported by funds from the Ministry of Education, University and Research (PRIN 2004).

## References

- [1] T. Katajama, A. Aoki, T. Nishimi, T. Okayama, *Measurement of Structural Properties of Riders*, JSAE paper 871229 (1987).
- [2] V. Cossalter, A. Doria, R. Lot, *Steady Turning of Two-Wheeled Vehicles*, *Vehicle System Dynamics*, Vol. 31, Swets & Zeitlinger (1999), pp 157-181.
- [3] V. Cossalter, R. Lot, F. Maggio, *The Modal Analysis of a Motorcycle in Straight Running and on a Curve*, *Meccanica*, Vol 39, Kluwer Academic Publishers (2004), pp.1-16.
- [4] V. Cossalter, A. Doria, s. Garbin, R. Lot, *Frequency-domain method for evaluating the ride comfort of a motorcycle*, *Vehicle System Dynamics*, Vol. 44, No. 4, Taylor&Francis (2006), pp. 339–355.

- 
- [5] R. Lot, V. Cossalter, M. Massaro, *The Significance of Frame Compliance and Rider Mobility on the Motorcycle Stability*, *Proceedings of Multibody Dynamics 2005, International Conference on Advances in Computational Multibody Dynamics-ECCOMAS Thematic Conference*, Madrid 21-24 June 2005.
- [6] H. Imaizumi, T. Fujioka, M. Omae, *Rider Model by Use of Multibody Dynamics Analysis*, Technical Notes, JSAE Review 17 (1996), pp 65-77.
- [7] V. Cossalter, *Motorcycle Dynamics*, Race Dynamics, Greendale WI, 2002.
- [8] T. Koizumi, N. Tsujiuchi, A. Tanaka: *Investigation on Riding Comfort and Stability Analysis on Vibration Input for Motorcycles*, *Proceedings of ISMA 2004, Leuven, Belgium, 20-22 september 2004*, pp. 2025-2034.
- [9] G. Höhne, *Computer Aided Development of Biomechanical Pilot Models*, Aerospace Science and Technology, Vol. 4, Elsevier (2000), pp 57-69.
- [10] H. Duda, G. Duus, G. Hovmark, L. Forssell, *New Flight Simulator Experiments on Pilot-Involved Oscillations due to Rate Saturation*, *Journal of Guidance, Control and Dynamics*, Vol 23, No. 2, AIAA (2000), pp 312-318.